International Journal of Environmental Sciences
ISSN: 2229-7359
Vol. 11 No. 13s, 2025
https://www.theaspd.com/ijes.php

Hybrid-Precision GNSS Positioning Strategies for Landslide Monitoring

Thanh Trung Duong[1], Nguyen Quoc Long[2], Bui Van Duc[3]
[1,2]Faculty of Geomatics and land Administration, Hanoi University of Mining and Geology, Vietnam
[3]Faculty of Civil Engineering, Hanoi University of Mining and Geology, Vietnam
[1]duongthanhtrung@humg.edu.vn

Abstract
Global Navigation Satellite System (GNSS) is now widely applied for early warning of natural hazards such as landslides. Given the required accuracy at the millimeter or centimeter level, networks of GNSS receivers with static surveying have been widely adopted for deformation monitoring. However, the primary limitation of static networks is that they typically require post-processing. In contrast, GNSS RTK enables to provide near real-time solution but has limitation in accuracy. To overcome these limitations, a hybrid GNSS positioning strategy have been proposed. In this approach, multi-function GNSS receivers are used and setup to implement both the GNSS RTK function and output raw data for accurate post processing. While GNSS RTK can provide displacement parameters at the centimeter level at frequency of 1Hz for early warning of natural hazards in the case of seriously landslide, post-processing, with network adjustment, provides accurate positioning solution in frequency of some hour for long term monitoring and reliable assessment of risk. Advanced data streaming, management and processing are also introduced in this study. The result from experiment and on-site project demonstrated the advantages of the hybrid strategy, which allowing for both real-time warning in the case of emergency landslide and accurate long-term risk deformation monitoring.
Keywords: *GNSS RTK · Post-Processing · Landslide Monitoring · Network Adjustment · Extended Kalmal Filter · RTK Network.*

1 INTRODUCTION

Landslides are natural disasters that pose endanger human lives, infrastructure, and ecosystems. Effective monitoring and early warning systems are crucial for mitigating these risks and improving response strategies. Global Navigation Satellite System (GNSS) technology has emerged as a vital tool in the field of landslide monitoring, offering high-precision positioning capabilities that facilitate the analysis of ground movement.Over the past decades, numerous studies have demonstrated the application of GNSS for landslide monitoring. For instance, [1] utilized GNSS Real-Time Kinematic (RTK) to monitor slope instability and achieve sub-centimeter accuracy in displacement detection. Similarly, [2] implemented GNSS post-processing techniques for long-term monitoring, showing their potential to capture millimeter-scale displacements. Moreover, [3] integrated GNSS data with geotechnical sensors to enhance the reliability of early warning systems, highlighting the complimentary strengths of these approaches.

GNSS Real-Time Kinematic (RTK) systems are particularly advantageous for landslide monitoring due to their ability to provide immediate data with high spatial and temporal resolution [4]. This makes RTK suitable for early warning applications where rapid response is critical. GNSS RTK is effective in detecting small-scale ground movement, which is critical for early warning systems in landslide monitoring. Even minute movements can be detected, which could indicate the potential for more significant shifts, helping in proactive mitigation ([5]; [6]). In addition, GNSS RTK's capability to monitor extensive regions is a significant advantage over other deformation monitoring methods like traditional surveying or inclinometers, which are more localized [7]; [8].Aside from its advantages, RTK also has limitations in the landslide monitoring. Landslide-prone areas often involve steep slopes or dense vegetation, which can block or degrade GNSS signal reception, leading to gaps in data and potential inaccuracies [9]; [10]. GNSS systems can be affected by adverse weather conditions such as heavy rain or snow, which can interfere with signal quality and cause interruptions in monitoring [11]; [12]. Above issue is particularly problem

in GNSS RTK when it may cause the confusion between positioning error and true displacement.
GNSS RTK often rely on stable reference stations and uninterrupted data transmission, which can be challenging in remote or unstable terrains ([13]).On the other hand, GNSS post-processing techniques, such as Precise Point Positioning (PPP) or network solutions, are well-suited for capturing long-term trends in landslide deformation. They offer high accuracy and are less dependent on real-time communication infrastructure [14]. However, the delay in obtaining results and the requirement for extensive computational resources limit their utility for immediate warning purposes [15]. One of the primary benefits of GNSS static post-processing is its ability to achieve millimeter-level accuracy, making it highly suitable for detecting minute displacements associated with slow-moving landslides. Unlike real-time techniques, static post-processing is less affected by short-term signal interruptions, as data can be reprocessed to mitigate errors caused by environmental factors or hardware issues [16].Another advantage is its adaptability to remote or inaccessible areas. In areas without real-time monitoring infrastructure, such as stable reference stations or reliable data transmission, static post-processing can still provide accurate displacement measurements by processing raw GNSS data after collection [4]. This flexibility makes it a valuable tool for monitoring landslides in challenging terrains and environments.
Despite its strengths, GNSS static post-processing also has notable limitations. One major drawback is the time delay in obtaining results, as data must be collected, transferred, and processed before meaningful displacement information is available [14]. This delay makes static post-processing unsuitable for applications requiring real-time or near-real-time decision-making, such as early warning systems for fast-moving landslides [17].Additionally, static post-processing requires high-quality raw GNSS data, which can be difficult to obtain in environments with dense vegetation, steep slopes, or significant atmospheric disturbances. These factors can degrade signal quality, leading to inaccuracies in the computed displacements [18]. Furthermore, the method typically involves longer observation periods, which may not be feasible for monitoring rapidly evolving landslide dynamics.Lastly, the complexity of post-processing workflows and the requirement for specialized software and expertise can be barriers for some users, particularly in regions with limited technical resources [19].Despite the demonstrated effectiveness of GNSS technologies, challenges remain in balancing the trade-offs between real-time monitoring and post-processing accuracy, particularly in the context of landslide-prone regions. This paper aims to explore these trade-offs and discuss the integration of GNSS RTK and post-processing techniques for optimizing landslide monitoring and early warning systems.

2 METHODOLOGY

The methodology of this study focuses on developing and validating a hybrid GNSS positioning framework that integrates Real-Time Kinematic (RTK) and post-processing network solutions for landslide monitoring.

2.1 Study Area Selection.

The study area is located in Quang Hanh Ward, Quang Ninh Province, in the northeast of Vietnam (Figure 1). The landslide occurred in this area due to the impact of a major storm namely Typhoon Yagi taken placed in September 2024). After the storm, there was a serious landslide and subsidence, causing many structural elements of buildings around that location to crack. The study area has a large slope, is located in an area of strong geological activity and has been excavated for construction, so it is vulnerable to extreme weather conditions such as storms and earthquakes. Due to the impact of prolonged heavy rain, certain facilities on the ground surface and many houses have serious subsidence, subsidence, and cracking, endangering the safety and property of many residents. Therefore, the necessary and urgent actions is to instantaneously assess specifically as well as monitor the level of surface displacement over time, thereby providing appropriate remedial measures.

International Journal of Environmental Sciences
ISSN: 2229-7359
Vol. 11 No. 13s, 2025
https://www.theaspd.com/ijes.php

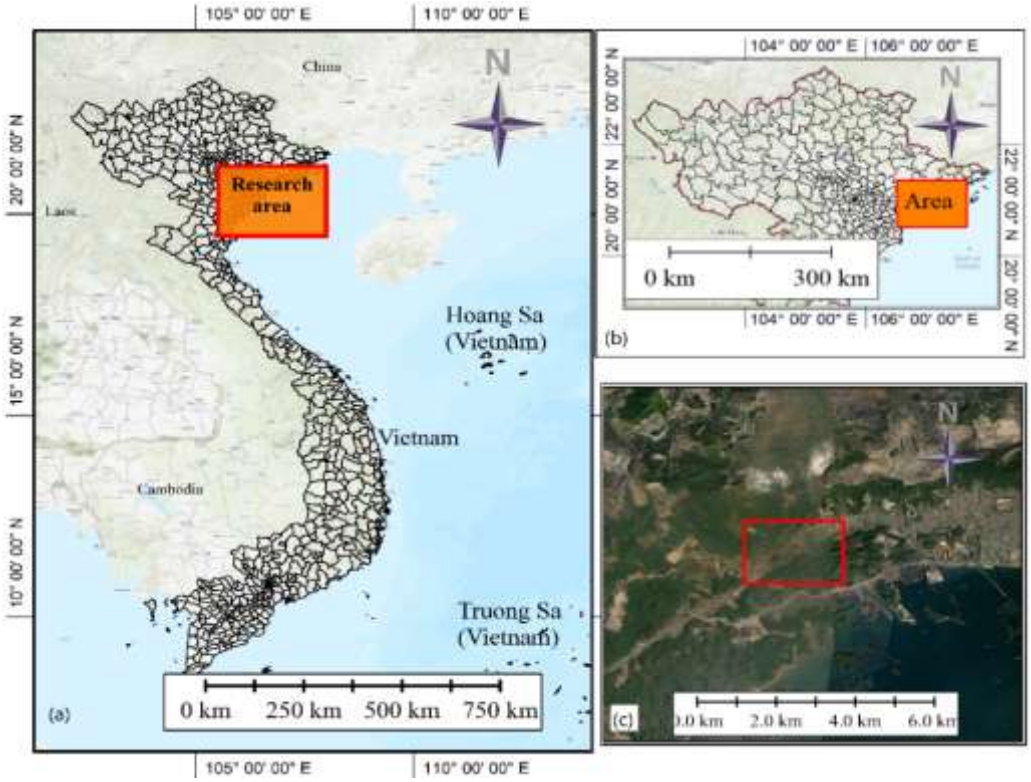

Fig. 1. (a) Location of the research area in Vietnam; (b) Location of the test site; (c) Image of the test site

2.2 GNSS Design and setup

To monitor the surface displacement, a network consists of a base station (reference station) and eight monitoring stations. The base station was installed at a location with stable geological foundation, far away from and not affected by landslides. Monitoring stations were placed at locations showing the most apparent signs of landslides to record coordinate changes during the observation period (Figure 2).

The equipment's used in the monitoring were dual-function multi-frequency GNSS receivers, in which the device can operate in Realtime Kinematic Positioning (RTK) mode to provide real-time coordinates of the stations and can also output RTCM (Radio Technical Commission for Maritime Services) data for post-processing. The transmission of data from the reference station to the monitoring stations and data from the monitoring stations to the server was carried out via the NTRIP (Networked Transport of RTCM via Internet Protocol). This is a common data transmission method in RTK measurements. It has the advantage of ensuring continuity, simple operation, suitable for a variety of terminal devices because it is developed based on the pure TCP/IP principle. The data logger was employed to receive RTCM data from the Base station and pushed those data to the monitoring stations to operate RTK measurement, and at the same time it collecting data from GNSS receivers in the field, then transmit the data to the server via the 4G wireless network using the NTRIP. The monitoring stations receive data from the reference station to measure RTK with an output frequency of 1Hz and centimeter-level accuracy for the fixed solution. This data helps to promptly report and warn in the case of landslides of medium and large magnitude in near real-time. On the other hand, the RTCM data of the measuring stations and the base station, after each cycle of several tens of minutes to several hours, is converted into RINEX format (Receiver Independent Exchange Format), and the spatial baseline between the stations is calculated to form a network. Network adjustments are performed to obtain coordinates of monitoring points with millimeter accuracy. This data is used to assess small surface movements and to inform long-term landslide reports.

International Journal of Environmental Sciences
ISSN: 2229-7359
Vol. 11 No. 13s, 2025
https://www.theaspd.com/ijes.php

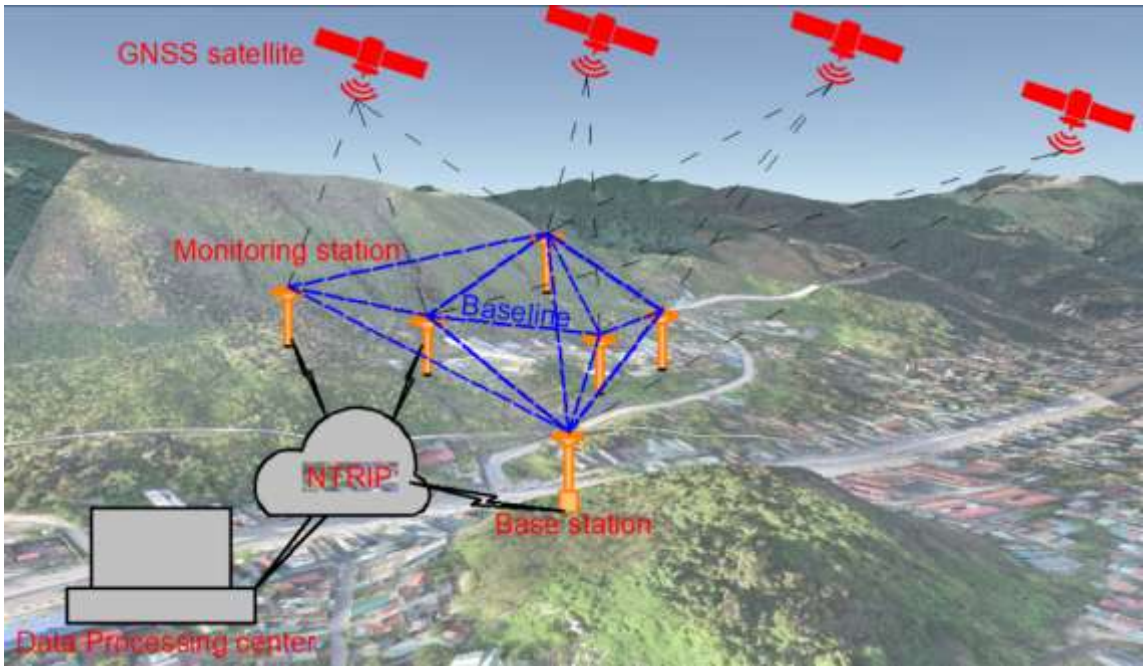

Fig. 2. GNSS design and setup used in this study

2.3 Hybrid GNSS Positioning Strategy

The hybrid positioning solution is illustrated in Figure 3. The calculation process consists of three main steps, each corresponding to a specific report.In the first step, the reference station continuously transmits RTCM correction data to the server via the NTRIP server protocol. The monitoring stations receive RTCM data from the reference station using the NTRIP client protocol, process the data, and output the RTK solution to a data logger. Additionally, the GNSS receivers at the monitoring stations generate RTCM data, which is sent back to the server along with the RTK solution. It should be noted that this feature is only available in new-generation GNSS modules or receivers equipped with moving base functionality, such as the u-blox ZED-F9P or Unicore UM982. The NTRIP caster software on the server manages user accounts and ensures data transmission between the base station and monitoring stations while also storing RTCM data from GNSS receivers for high-precision post-processing.In the second step, the RTCM data from the monitoring stations is converted into RINEX format after a defined time interval, typically ranging from one to several hours. Baseline computations between stations are then performed to establish a network. The residual measurements in the network allow for the assessment of spatial triangle closure errors to control measurement accuracy. Through a network adjustment solution based on the least squares principle, high-precision point coordinates (on the millimeter level) can be obtained. Theoretically, any two stations recording data simultaneously can form a baseline. In a monitoring network, where stations continuously and simultaneously collect data, the number of measurements in the network can become very large as the number of monitoring stations increases, leading to a significant processing workload. To address this issue, only selected baselines are included in an optimized configuration, ensuring network rigidity for improved positioning accuracy while preventing data processing overload to allow for timely reporting.In the third step, the RTK measurements and the adjusted results from post-processing are combined using an Extended Kalman Filter to enhance the predictive accuracy of RTK solutions. The mathematical model is designed and elaborated in the following sections can be seen in the [20].

International Journal of Environmental Sciences
ISSN: 2229-7359
Vol. 11 No. 13s, 2025
https://www.theaspd.com/ijes.php

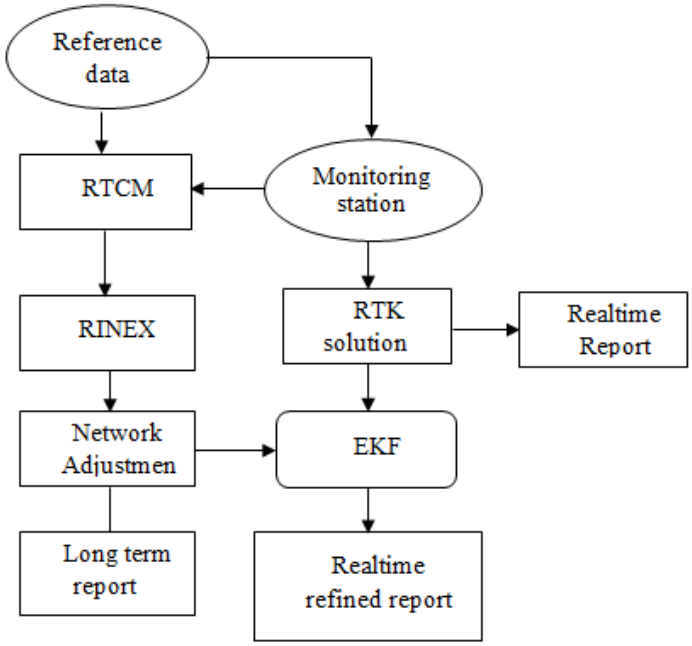

Fig. 3. Flow chart of the data analysis in the hybrid GNSS positioning system

3. VALIDATION AND PERFORMANCE ASSESSMENT

To standardize and evaluate the accuracy of the proposed the coupled GNSS RTK/post-processing method before applying it in practice, a model consisting of four points including one reference station and three monitoring stations was established (Figure 4). The displacement of the monitoring stations was simulated by intentionally shifting the reference station coordinates by 5 mm along each axis per iteration. Theoretically, when the reference station is shifted, the coordinates of the monitoring stations should change by the same amount. Based on this principle, the observed displacements serve as a basis for assessing the accuracy of the proposed methods, including static measurements and RTK measurements.At each instance of reference station coordinate adjustment, RTK measurements were performed while simultaneously collecting RTCM data for static processing over different time intervals. The measurement results were then analyzed to evaluate accuracy of the evaluating methods. Table 1 presents the static measurement coordinates and their corresponding standard deviations in the local coordinate system (UTM projection) for various measurement durations. Table 2 provides an accuracy analysis of horizontal and vertical displacement.

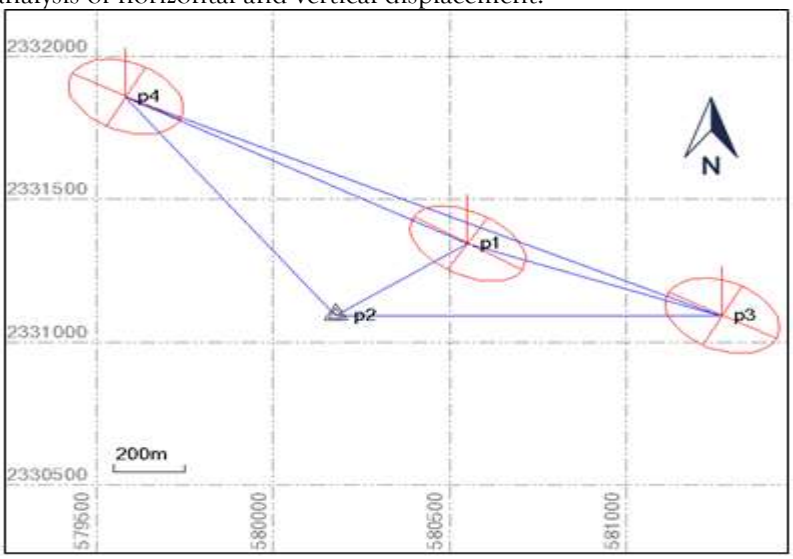

Fig. 4. Preliminary experimental testing network.

International Journal of Environmental Sciences
ISSN: 2229-7359
Vol. 11 No. 13s, 2025
https://www.theaspd.com/ijes.php

Table 2. Numerical analysis of network adjustment results.

Section number	Point ID	Easting (m)	Easting Error (m)	Northing (m)	Northing Error (m)	Elevation (m)	Elevation Error (m)
Duration (minutes)							
Sec1	P1	580551.538	0.001	2331343.312	0.001	17.588	0.003
180	p2	580178.102	-	2331091.376	-	27.91	-
11h59-	p3	581271.514	0.001	2331089.368	0.001	26.949	0.003
14h59	p4	579582.033	0.001	2331857.018	0.001	27	0.003
Sec2	P1	580551.545	0.002	2331343.315	0.001	17.598	0.005
66	p2	580178.107	-	2331091.381	-	27.915	-
9h29-	p3	581271.519	0.002	2331089.372	0.002	26.956	0.005
10h35	p4	579582.043	0.002	2331857.023	0.002	27.014	0.005
Sec3	p1	580551.548	0.001	2331343.318	0.001	17.599	0.003
86	p2	580178.115	-	2331091.385	-	27.92	-
16h26-	p3	581271.520	0.001	2331089.381	0.001	26.948	0.003
17h52	p4	579582.054	0.001	2331857.025	0.001	27.029	0.003
Sec4	p1	580551.554	0.004	2331343.322	0.003	17.597	0.014
40	p2	580178.120	-	2331091.391	-	27.925	-
15h20-	p3	581271.529	0.004	2331089.384	0.004	26.978	0.017
16h00	p4	579582.060	0.004	2331857.028	0.004	27.034	0.016
Sec5	P1	580551.558	0.005	2331343.326	0.004	17.623	0.010
69	P2	580178.125	-	2331091.396	-	27.93	-
16h30-	p3	581271.534	0.010	2331089.392	0.006	26.972	0.017
17h39	p4	579582.063	0.009	2331857.032	0.005	27.032	0.014

Table 2. Displacement error of static surveying.

Section number	Point ID	Northing Disp (m)	Easting Disp (m)	Elevation Disp (m)	Northing Disp Error (m)	Easting Disp Error (m)	Elevation Disp Error (m)
Duration (minutes)							
Sec2	P1	0.007	0.003	0.01	0.002	-0.002	0.005
66	p3	0.005	0.004	0.007	0.000	-0.001	0.002
	p4	0.010	0.005	0.014	0.005	0.000	0.009
Sec3	p1	0.003	0.003	0.001	-0.002	-0.002	-0.004
86	p3	0.001	0.009	-0.008	-0.004	0.004	-0.013
	p4	0.011	0.002	0.015	0.006	-0.003	0.010
Sec4	p1	0.006	0.004	-0.002	0.001	-0.001	-0.007
40	p3	0.009	0.003	0.03	0.004	-0.002	0.025
	p4	0.006	0.003	0.005	0.001	-0.002	0.000
Sec5	P1	0.004	0.004	0.026	-0.001	-0.001	0.021
69	p3	0.005	0.008	-0.006	0.000	0.003	-0.011
	p4	0.003	0.004	-0.002	-0.002	-0.001	-0.007
STD					0.003	0.002	0.012
Max Error					0.006	0.004	0.025

International Journal of Environmental Sciences
ISSN: 2229-7359
Vol. 11 No. 13s, 2025
https://www.theaspd.com/ijes.php

The results in Table 1 indicate that to achieve millimeter-level accuracy in both horizontal and vertical positioning, the static measurement duration should exceed 60 minutes. The displacement error assessment in Table 2 shows that the horizontal accuracy is approximately 2–3 millimeters, while the vertical accuracy is around 12 millimeters. Significant errors were observed in sections 4 and 5, with corresponding values of 0.025 m and 0.021 m. This demonstrates the consistency between the accuracy evaluation from the adjustment results and the assessment based on true errors. The results also show that parts with measurement durations of less than 60 minutes and those recorded in the midday or afternoon hours lowered measurement accuracy due to the ionospheric effects ([21], [22]).
During the static data collection period, RTK data was also recorded at point P1 at a sampling rate of approximately one measurement every 10 seconds. The displacement accuracy of RTK measurements compared to the intentional displacement was analyzed and is presented in Figures 5, 6, 7, and 8, respectively. These correspond to the errors in the North, East, and Height in sections 2, 3, 4, and 5. Statistical analyses are presented in the table 3.

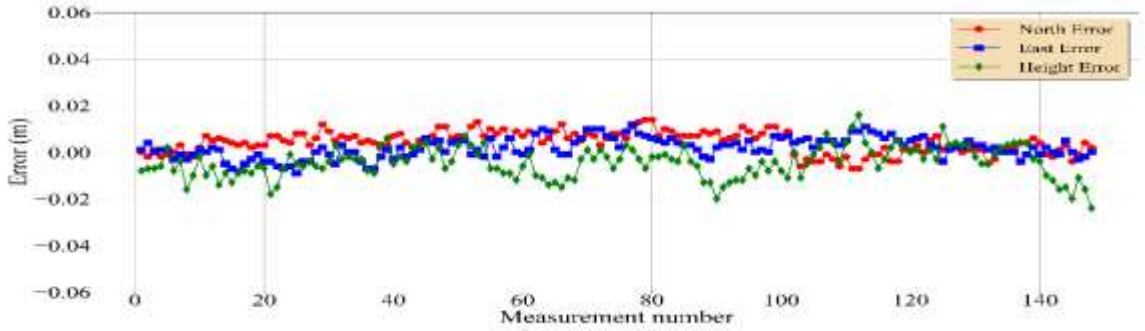

Fig. 5. Displacement error of the RTK measurements in the section 2.

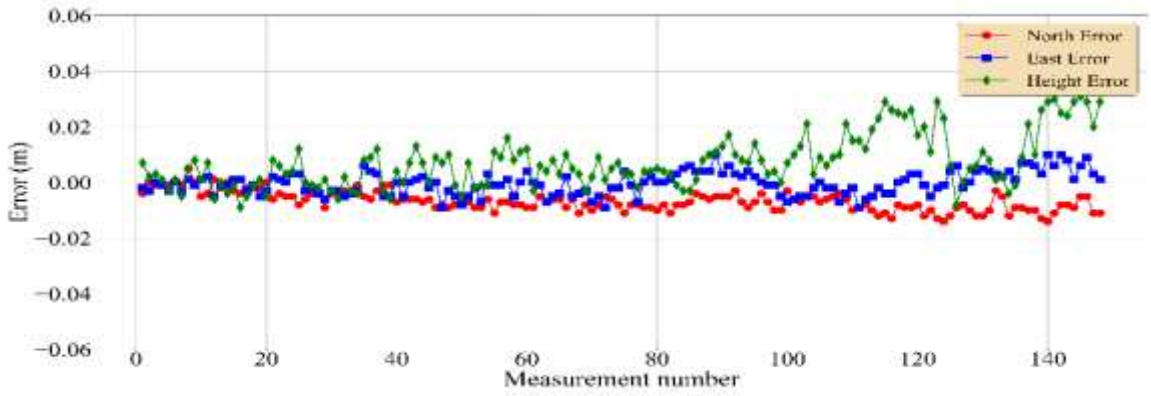

Fig. 6. Displacement error of the RTK measurements in the section 3.

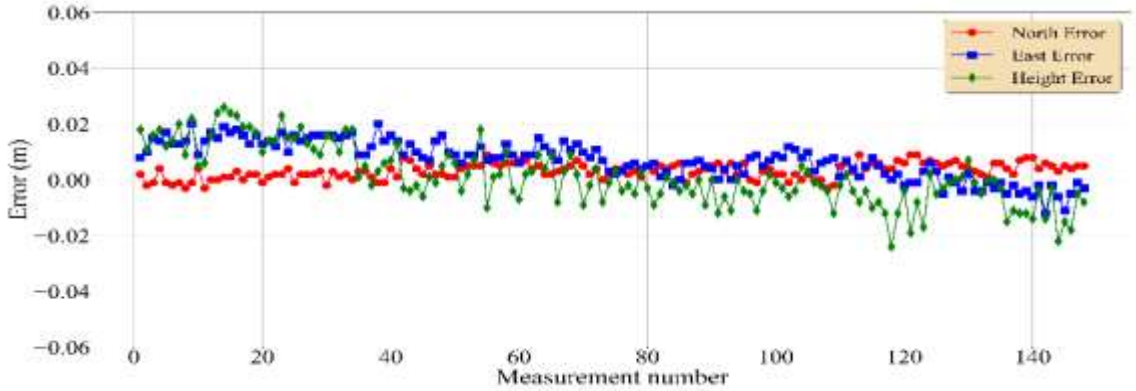

Fig. 7. Displacement error of the RTK measurements in the section 3

International Journal of Environmental Sciences
ISSN: 2229-7359
Vol. 11 No. 13s, 2025
https://www.theaspd.com/ijes.php

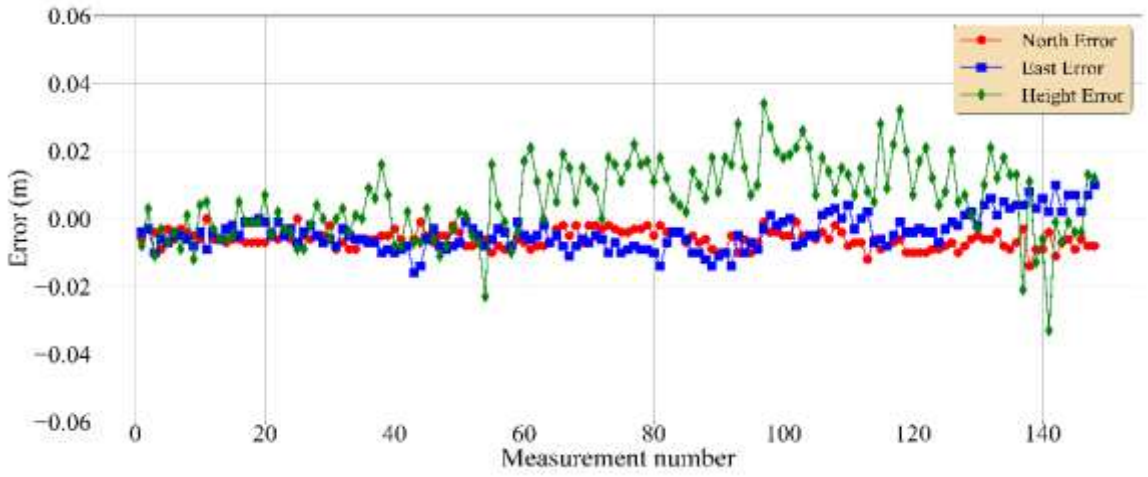

Fig. 8. Displacement error of the RTK measurements in the section 4

Table 3. Numerical analysis of the point P1

Sections	Nstd (m)	Estd (m)	Hstd (m)	Nmax error (m)	Emax Error (m)	Hmax Error (m)
Sec2	0.005	0.004	0.007	0.014	0.012	-0.024
Sec3	0.003	0.004	0.009	-0.014	0.010	0.031
Sec4	0.003	0.007	0.010	0.009	0.020	0.026
Sec5	0.003	0.005	0.011	-0.014	-0.016	0.034

The statistical data in Table 3 shows that GNSS RTK measurements have a positional standard deviation ranging from 3–7 millimeters in horizontal and approximately 11 millimeters in vertical. This indicates that the horizontal accuracy of RTK measurements is lower compared to static measurements. The vertical accuracy of RTK measurements is comparable to the height accuracy in static measurements for some sections with short observation durations (<60 minutes). However, it can be observed that the dispersion or maximum error in RTK measurements is larger, which reduces the reliability of RTK measurements compared to static measurements. Statistical analyses also show that RTK measurements taken in the morning (Section 2) have higher accuracy than those taken in the afternoon. This result is in agreement with previous works [21], [22]

4. FIELD INSTALLATION AND LANDSLIDE MONITORING

4.1 Equipment's Used

Dual frequency, multi-functions GNSS RTK receivers developed based on the Ublox F9P module, were used for monitoring. The specification of the GNSS receiver is described in Table 4.

Table 4. Specification of the testing device.

Satellite constellation	GPS (L1C/A, L2C) GALLIEO (E1-B/C, E5b) GLONASS (L1OF, L2OF) BEIDOU (B1, B2) QZSS
Output frequency	1 Hz
RTK Accuracy	Vertical: 0.8 m + 1ppm, Horizontal: 1.5 cm + 1ppm
Statics Surveying	Vertical: 3 mm + 0.5ppm, Horizontal: 5 mm + 0.5ppm

International Journal of Environmental Sciences
ISSN: 2229-7359
Vol. 11 No. 13s, 2025
https://www.theaspd.com/ijes.php

4.2 Field Implementation

The installation layout of the monitoring stations is shown in Figure 9. It includes eight GNSS monitoring stations labeled from GNSS01 to GNSS08 and one reference station (Base GNSS). Representative images of the reference and monitoring stations are presented in figures 10. The distance between the two nearest monitoring stations is 20 (m) and the farthest is 398 (m). The farthest distance from the reference station to the monitoring station is 406 (m). The average distance between monitoring stations is 120 (m).

Fig. 9. Diagram of the sensors installed

Fig. 10. Images of Reference station (Left) and monitoring station (right)

4.3 Analysis of monitoring data

Field measurements were evaluated on-site, and those did not meet the standards were discarded and replaced with new ones. Standard-compliant measurements were weighted-averaged to obtain the best results.The coordinate and elevation values (N, E, H) of the monitoring points were used to calculate the horizontal displacement parameters, vertical displacement, velocity, and direction of movement.Horizontal displacement along the N and E axes was estimated as follows:

$$dN = N_{n+1} - N_n \quad (1)$$

$dE = E_{n+1} - E_n$ (1)

Total horizontal displacement ΔD:

$\Delta D = \sqrt{dN^2 + dE^2}$ (3)

Vertical displacement dH:

$dH = H_{n+1} - H_n$ (4)

Horizontal displacement velocity:

$V_D = \Delta D / \Delta T$ (5)

Vertical displacement velocity:

$V_H = dH / \Delta T$ (6)

where ΔT is the time interval between two observation cycles.

Since measurement data may contain observational errors, the magnitude and velocity of displacement at monitoring locations are evaluated using the standard deviation to determine actual displacement levels and rates. The threshold for identifying significant displacement is calculated using the following equation:

$V_H = dH / \Delta T$ (7)

where V_t is the threshold value, and STD is the standard deviation of measurements.

Using equation (7), any measured values exceeding the threshold are considered to indicate displacement with a 99% probability. The displacement velocity is then compared with the classification table in Table 5 to determine the warning level for landslides [23].

Table 5. Velocity Classes [23].

Classify	m/year	m/month	m/day	m/hour	m/minute	m/sec	mm/sec
Extremely rapid					300	5	5000
Very rapid				180	3	0.05	50
Rapid			43.2	1.8	0.03	0.0005	0.5
Moderate	157.68	12.96	0.432	0.018	0.0003	0.000005	0.005
Slow	1.5	0.013	0.000432	0.000018	3 x 10-7	3 x 10-9	5 x 10-5
Very Slow	0.017	0.0014					

4.4 Monitoring result report

The monitoring results over a specific period are generated into reports depending on the landslide velocity of the study area. In the case of the monitored area in this study, the landslide velocity is assessed as slow or very slow. Therefore, reports are generated on a daily cycle. The table 6 presents the monitoring report at a specific point over 18 days. Figures 11 and 12 graphically represent the corresponding data.

Table 6. Displacement report of GNSS02

No	Time	dN(m)	dE(m)	dH(m)	vH (m/day)	vD (m/day)
1	Nov 28, 2024					
2	Nov 29, 2024	0.002	0.005	0.008		
3	Nov 30, 2024	0.002	0.005	0.009	0.009	0.006
4	Dec 1, 2024	0.003	0.006	0.009	0.009	0.007
5	Dec 2, 2024	0.004	0.007	0.009	0.009	0.007
6	Dec 3, 2024	0.004	0.007	0.010	0.010	0.008
7	Dec 4, 2024	0.005	0.008	0.011	0.011	0.009
8	Dec 5, 2024	0.005	0.008	0.011	0.011	0.009
9	Dec 7, 2024	0.006	0.008	0.011	0.006	0.005
10	Dec 8, 2024	0.006	0.008	0.011	0.011	0.010
11	Dec 9, 2024	0.007	0.009	0.012	0.012	0.011
12	Dec 10, 2024	0.000	-0.011	0.004	0.004	0.011
13	Dec 11, 2024	0.000	-0.006	0.007	0.007	0.006
14	Dec 12, 2024	-0.002	-0.005	-0.003	-0.003	0.006
15	Dec 13, 2024	-0.002	-0.006	-0.009	-0.009	0.007

16	Dec 15, 2024	0.002	-0.004	0.011	0.005	0.002
17	Dec 16, 2024	-0.001	-0.002	-0.006	-0.006	0.002
18	Dec 18, 2024	0.000	-0.011	0.004	0.002	0.005
STD	**0.003**	**0.008**	**0.007**	**0.007**	**0.003**	
Threshold	**0.010**	**0.023**	**0.021**	**0.020**	**0.009**	

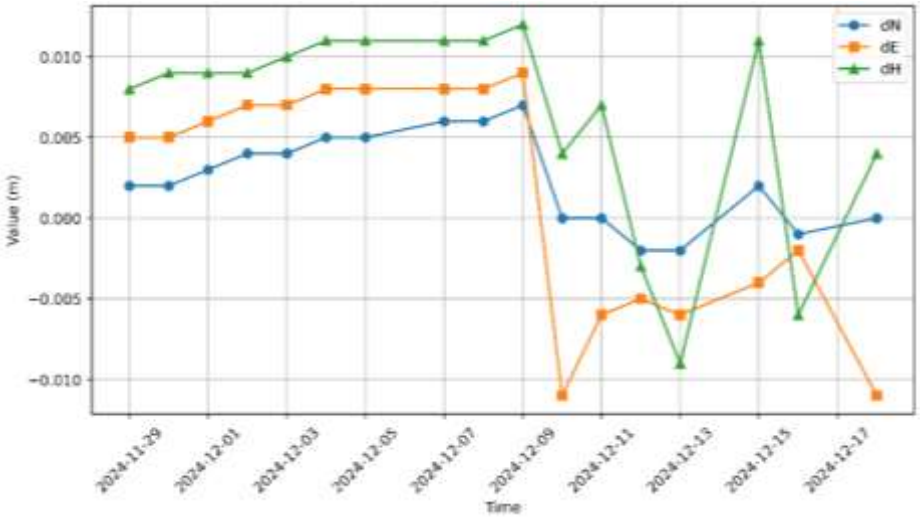

Fig. 11. Graphical displacement description of GNSS02

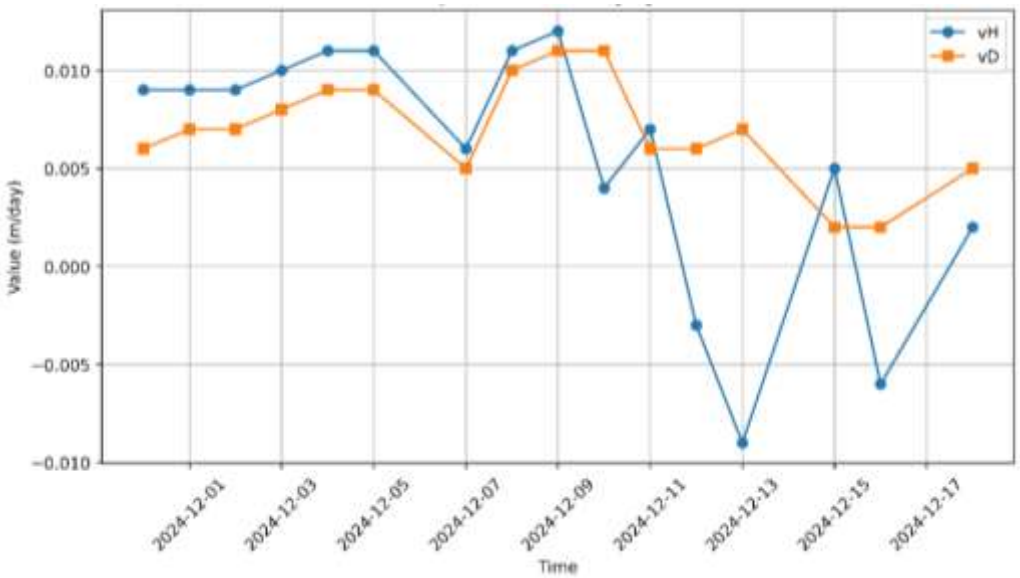

Fig. 12. Graphical description of displacement velocity at GNSS02

With the hybrid positioning method as presented, GNSS technology can monitor surface displacements within 2–3 centimeters in real time and at the millimeter level for daily reports. The report at point GNSS02 indicates that the displacement velocity at the observed point falls into the slow or very slow compared with the standard in Table 5.

4 CONCLUDING REMARK

This study proposes a hybrid solution combining two GNSS positioning methods: real-time kinematic (RTK) positioning and post-processed static measurement. The goal is to leverage the advantages and mitigate the disadvantages of each method when used independently, taking advantage of advancements in the latest generations of GNSS receivers. This approach enables the timely reporting of significant surface displacements in cases of moderate to severe landslides while also providing reports for slow and

very slow landslide events.

One of the key advantages of using GNSS technology for landslide monitoring is its ability to cover a wide range of areas, from small scales (tens of meters) to large scales (several kilometers), without requiring significant additional investment. However, a limitation of this method is its dependence on environmental conditions and observation timing. The placement of GNSS antennas must be in an open area to receive the maximum number of satellite signals, and data collection should be conducted in the morning (local time) to ensure the highest accuracy in reporting.

Experiments and analyses indicate that the hybrid positioning solution, combining GNSS RTK with selective network adjustment in post-processing, can be effectively applied to monitor subsidence and landslides caused by extreme weather events. This solution can also be used to monitor the stability of large-scale artificial structures.

ACKNOWLEDGEMENT

The authors give a great appreciation to all contributors, authors, reviewers and editor for supporting this work.

REFERENCES

[1] Y. X. C. &. S. W. Zhang, "Real-time landslide monitoring using GNSS RTK technology: Case studies and performance analysis," Journal of Geodetic Science, vol. 25, no. 3, pp. 135-148, 2019.

[2] J. H. J. &. W. T. Li, "Post-processing techniques for long-term GNSS-based landslide monitoring," Landslides, pp. 17(4), 811-824, 2020.

[3] J. P. S. &. L. H. Suh, "Integration of GNSS and geotechnical sensors for improved landslide early warning systems," Geomatics, Natural Hazards and Risk, pp. 12(2), 456-471, 2021.

[4] J. A. C. J. &. R. J. Gili, "Advantages and limitations of GNSS RTK in landslide monitoring applications," Engineering Geology, pp. 266, 105479, 2020.

[5] G. Q. Wang, "Millimeter-accuracy GPS landslide monitoring," Journal of Geodetic Science, pp. 3(1), 22-31, 2013.

[6] C. P. W. L. K. L. Wang Xin, "Landslide surface horizontal displacement monitoring based on image recognition technology and computer vision,," Geomorphology, pp. 431(15), 108691, 2023.

[7] L. X. K. G. X. e. a. Yu, "Application of GNSS-PPP on Dynamic Deformation Monitoring of Offshore Platforms," China Ocean Eng, pp. 38, 352–361, 2024.

[8] L. P. T. I. M. Yehuda Bock, "Detection of arbitrarily large dynamic ground motions with a dense high-rate GPS network," Geophysical Research Letters, p. 31(6), 2004.

[9] J. Han, R. Tu, R. Zhang, L. Fan and P. Zhang, "SNR-Dependent Environmental Model: Application in Real-Time GNSS Landslide Monitoring," Sensors, pp. 19(22), 5017, 2019.

[10] C. Jing, G. Huang, Q. Zhang, X. Li, Z. Bai and Y. Du, "GNSS/Accelerometer Adaptive Coupled Landslide Deformation Monitoring Technology," Remote Sensing, p. 14(15):3537, 2022.

[11] Y. e. a. Zhang, "GNSS techniques for real-time monitoringof landslides: a review," Satellite Navigation, pp. 4(5), 1-10, 2023.

[12] A. Parker, W. Featherstone, N. Penna, M. Filmer and M. Garthwaite, "Practical Considerations before Installing Ground-Based Geodetic Infrastructure for Integrated InSAR and cGNSS Monitoring of Vertical Land Motion.," Sensors, pp. 17, 1753, 2017.

[13] T. &. W. B. Günther, "Standalone and RTK GNSS applications in remote and unstable terrains: Lessons learned.," Inside GNSS, pp. 11(4), 45-52, 2018.

[14] Y. &. L. Z. Feng, "Precise Point Positioning for long-term landslide deformation monitoring," Geophysical Journal International, , pp. 210(2), 935-947, 2017.

[15] X. C. Q. &. W. S. Dong, "Comparative analysis of real-time and post-processed GNSS data in landslide monitoring.," Natural Hazards and Earth System Sciences, pp. 21(1), 123-134., 2021.

[16] J. H. J. &. W. T. Li, "Post-processing techniques for long-term GNSS-based landslide monitoring.," Landslides, vol. 17, no. 4, pp. 811-824., 2020.

[17] C. e. a. Xu, "Degradation of GNSS signals in complex landslide environments.," Remote Sensing, vol. 14, no. 15, p. 3537, 2021.

[18] P. e. a. Brunet, "Challenges of GNSS signal reception in mountainous and vegetated regions for deformation monitoring.," Sensors, vol. 19, no. 22, p. 5017, 2016.

[19] C. e. a. Werner, "Atmospheric effects on GNSS signal propagation in severe weather conditions.," Sensors, vol. 17, no. 8, p. 1753, 2017.

[20] T. Duong, "Real-Time Deformation Monitoring with Clustered GNSS RTK Networks: An Advanced CORS Approach for Structural Stability Analysis," in Bui, D.T., Hoang, A.H., Le, T.T., Vu, D.T., Raghavan, V. (eds) Geoinformatics for Spatial-Infrastructure Development in Earth and Allied Sciences. GIS-IDEAS 2023. Lecture Notes in Civil Engineering, Hanoi, Vietnam, Springer, Cham, 2024, p. 411.